Biomaterials 31 (2010) 5408–5417

Contents lists available at ScienceDirect

Biomaterials

journal homepage: www.elsevier.com/locate/biomaterials

Porous nanocrystalline silicon membranes as highly permeable and molecularly thin substrates for cell culture

A.A. Agrawal [a], B.J. Nehilla [a], K.V. Reisig [b], T.R. Gaborski [a,1], D.Z. Fang [c], C.C. Striemer [c,1], P.M. Fauchet [c], J.L. McGrath [a,*]

[a] Department of Biomedical Engineering, University of Rochester, Rochester, NY 14627, USA
[b] SiMPore Inc., Rochester, NY 14627, USA
[c] Department of Electrical and Computer Engineering, University of Rochester, Rochester, NY 14627, USA

ARTICLE INFO

Article history:
Received 8 March 2010
Accepted 16 March 2010
Available online 15 April 2010

Keywords:
Porosity
Silicon
Cell culture
Nanoporous
Cell adhesion
Biocompatibility

ABSTRACT

Porous nanocrystalline silicon (pnc-Si) is new type of silicon nanomaterial with potential uses in lab-on-a-chip devices, cell culture, and tissue engineering. The pnc-Si material is a 15 nm thick, freestanding, nanoporous membrane made with scalable silicon manufacturing. Because pnc-Si membranes are approximately 1000 times thinner than any polymeric membrane, their permeability to small solutes is orders-of-magnitude greater than conventional membranes. As cell culture substrates, pnc-Si membranes can overcome the shortcomings of membranes used in commercial transwell devices and enable new devices for the control of cellular microenvironments. The current study investigates the feasibility of pnc-Si as a cell culture substrate by measuring cell adhesion, morphology, growth and viability on pnc-Si compared to conventional culture substrates. Results for immortalized fibroblasts and primary vascular endothelial cells are highly similar on pnc-Si, polystyrene and glass. Significantly, pnc-Si dissolves in cell culture media over several days without cytotoxic effects and stability is tunable by modifying the density of a superficial oxide. The results establish pnc-Si as a viable substrate for cell culture and a degradable biomaterial. Pnc-Si membranes should find use in the study of molecular transport through cell monolayers, in studies of cell-cell communication, and as biodegradable scaffolds for three-dimensional tissue constructs.

1. Introduction

Nanoporous membranes are useful tools for cellular research. They are typically used to create 'transwell' devices to separate culture chambers into upper and lower compartments. By growing different cell types in each chamber, scientists maintain physical separation of the cells while allowing soluble factors to pass between chambers. Such arrangements are useful in the study of cell-cell communication [1,2] and for cultures where the growth of one cell type is dependent or enhanced by factors secreted from a second cell type [3,4]. The permeability of confluent cell monolayers to soluble factors is also studied using transwell devices [5]. For example, the ability of small molecules to pass culture models of the intestinal lining is one important indicator of the efficacy of drug candidates [6]. The membranes used in transwells are typically 'track-etched' membranes created by bombarding sheets of dense polycarbonate (PC) or polyester-sulfone (PES) with sub-atomic particles to fracture the polymer backbone. Chemical etching is then used to open up holes along fracture paths until pores are about 450 nm in diameter. This pore dimension prevents cells from migrating through the membranes but allows the free passage of soluble factors between compartments. Although pores can vary in shape through the ~ 10 um thickness of the track-etched (TE) membranes, they are relatively monodisperse except where pore overlap occurs [7].

Porous nanocrystalline silicon (pnc-Si) is a recently discovered membrane material [8] with many potential applications in biotechnology, including cell culture. The striking structural characteristic of pnc-Si that distinguishes it from all commercial membrane materials is its molecular thinness. Originally described as a 15 nm thick porous membrane [8], pnc-Si membranes have now been made with thicknesses ranging from 10 nm and 50 nm. Because the resistance to transport scales directly with membrane thickness, the fact that pnc-Si membranes are ~ 1000 thinner than commercial membranes implies permeabilities that are orders of

* Corresponding author. Tel.: +1 585 273 5489.
E-mail address: jmcgrath@bme.rochester.edu (J.L. McGrath).
[1] Currently at SiMPore, Inc., West Henrietta, NY 14586, USA.

0142-9612/$ – see front matter © 2010 Elsevier Ltd. All rights reserved.
doi:10.1016/j.biomaterials.2010.03.041

magnitude higher. This expectation has now been confirmed experimentally for both diffusion [9] and convection [10] through pnc-Si. The pores in pnc-Si are created by inducing silicon crystal growth in an amorphous silicon layer and the temperature used to induce crystal growth determines the pore size distribution. Average pore sizes are tunable between 3 nm and 80 nm by adjusting the temperature of anneal and porosities can be as high as 15%. The membranes are made with inexpensive and scalable silicon manufacturing processes and allow for a variety of planar shapes and dimensions to be created. Macroscopic dimensions of freestanding membrane can withstand practical laboratory pressures without rupture.

Given the molecular thinness and high permeability of pnc-Si, we anticipate that the material will have value as a membrane material for cell culture. If a variety of cell types can be grown on pnc-Si, then co-culture devices could be created with pnc-Si membranes in which cells are physically separated by as little as 10 nm by a highly permeable barrier. Cell-cell signaling could be more robust under these conditions, particularly if mediated by low abundance molecules that are diluted or adsorbed using standard transwell materials and procedures. If pnc-Si is biodegradable, it could be used as a permeable template to seed different cell types and create stratified tissues *in vitro* without any intervening membrane or embedding material. Monolayer permeability studies might be done on pnc-Si with the advantage that the underlying membrane is orders of magnitude more permeable than commercial membranes and therefore less likely to contribute a resistance that can mask fast cellular transport processes. Another intriguing possibility is that the planar silicon format will allow for new devices that combine highly permeable membranes with microfluidics to enable time resolved studies of cellular responses to soluble factors delivered with precise temporal and spatial control.

To lay the foundation for these and other cellular applications, we must first address basic questions about the biocompatibility and biodegradation of pnc-Si. Because the outermost layer of pnc-Si is a glass-like $\sim$ 1 nm native silicon oxide that grows within hours after exposure to atmosphere [11], we hypothesized that pnc-Si will be as viable for cell culture as glass coverslips which are used routinely to grow cells for microscopic observations. We tested this hypothesis by quantifying the adhesion, growth and viability of both a robust immortalized cell line of mouse fibroblasts (3T3-L1) and a more environmentally sensitive primary culture of human umbilical vein endothelial cells (HUVEC) on pnc-Si, tissue culture plastic and glass. Given the chemical similarity of pnc-Si and porous silicon (PSi), we anticipated that pnc-Si would degrade in physiologic buffers in a non-toxic manner [12–14] and thus we also investigated pnc-Si dissolution behavior in cell culture media. The ability to control such degradation through surface modifications is important to opening the full range of possible applications of pnc-Si to cell culture. Other exciting applications of pnc-Si as a biomaterial include the potential to co-culture cells across an extremely thin porous membrane and the ability to use phase or fluorescence microscopy to monitor cellular signals through the transparent pnc-Si membrane. The feasibility of these potential applications was tested with pnc-Si and two populations of fluorescently-tagged white blood cells.

2. Materials and methods

2.1. Materials

Dulbecco's Modified Eagle Medium (DMEM), 0.25% Trypsin-EDTA, Fetal Bovine Serum (FBS), penicillin/streptomycin, glutamine, CellTracker Green 5-chloromethylfluorescein diacetate (CMFDA) and the Live/Dead Viability/Cytotoxicity Kit were purchased from Invitrogen (Carlsbad, CA USA). Cloning rings (6.4 mm inner diameter x 8 mm height) and poly-L-lysine (PLL) for cell culture were purchased from Sigma (St. Louis, MO USA). Methanol (MeOH), ethanol (EtOH), 22 mm^2 glass cover slips and all tissue culture-treated polystyrene (TCPS) were purchased from VWR.

2.2. Cell culture

Cell studies were performed with HUVEC (Microbiology & Immunology Lab, University of Rochester Medical Center, Rochester, NY, USA) and mouse embryo fibroblasts (3T3-L1, ATCC, Rockville, MD, USA). These cells were cultured at 37 °C in a 5% CO_2, 90% humidified atmosphere. HUVEC were grown in EGM (Lonza) with 2% L-glutamine, 1% penicillin/ streptomycin and 10% FBS, and 3T3-L1 were grown in DMEM with antibiotics and serum. Media was changed every other day. Cells were harvested after reaching 70–80% confluence by trypsinization with 0.25% trypsin-EDTA and subsequently seeded at appropriate densities. HUVEC and 3T3-L1 were used between passages 4–8 and 17–25, respectively.

2.3. Pnc-Si fabrication

Pnc-Si membranes were fabricated using standard semiconductor processes, as recently described [8]. Thermal oxide (1000 Å) was grown on both sides of a (100) n-type silicon wafer. The backside of the wafer was patterned using photolithography in order to form an etch mask for the membranes. During lithography, the frontside oxide was removed. A 3-layer film stack consisting of silicon dioxide (20 nm)/amorphous silicon (15 nm)/silicon dioxide (20 nm) was then deposited onto the bare silicon wafer by RF magnetron sputtering (ATC-2000V, AJA International, N. Scituate, MA). A Surface Science Integration (Solaris 150) Rapid Thermal Processing (RTP) system (El Mirage, AZ) was used to anneal the film stack to 1000 °C for 60 s and transform the amorphous silicon to a nanocrystalline state. The membrane was exposed by removing the bulk silicon using the preferential silicon etchant ethylenediamine pyrocatechol (EDP). Due to its high silicon to oxide etch selectivity, the EDP etch terminated at the first protective oxide layer in the membrane film stack. Finally, the protective oxide layers were etched with buffered oxide etchant (BOE), thus releasing the pnc-Si membrane. The mask was designed to yield approximately 80 samples per silicon wafer. Each sample contained two 2000 $\times$ 100 μm slits with freely suspended 15 nm thick pnc-Si membranes (Fig. 1).

2.4. Post-production thermal processing

Unless otherwise noted, pnc-Si samples underwent an additional post-production thermal processing step in the RTP unit before use in cell culture. Samples were placed on a silicon carbide-coated graphite susceptor and exposed to Argon gas. The temperature was increased at 10 °C/s to a steady state of 800 °C. Samples were maintained at 800 °C for 5 minutes, cooled to 25 °C and used without further processing.

2.5. Pnc-Si membrane stability in cell culture media

Pnc-Si membrane stability and chip discoloration were monitored for 7 days. To measure membrane stability, polystyrene cloning rings were attached to the membrane side of pnc-Si chips using silicone vacuum grease. The rings were then filled with DMEM culture media containing 15 μm polystyrene beads (FS07F, Bangs Laboratories). In this way, the cloning rings prevented polystyrene beads from rolling off the chips when culture dishes were moved. After allowing the beads to settle for $\sim$ 20 minutes, images were captured for over 30 hours at 25 °C to monitor membrane integrity *via* time-lapse phase contrast microscopy. Microscopy was performed with a 10X objective on a Nikon Eclipse TS-100F inverted microscope equipped with Cooke SensiCam cooled CCD camera.

To measure discoloration, pnc-Si samples were sterilized with MeOH and then incubated in serum-supplemented DMEM under cell culture (37 °C, 5% CO_2, 90% humidity) conditions or at room temperature. Once a day, samples were removed from the incubator, rinsed in DIH_2O and 70% EtOH, imaged with a Canon Powershot A650IS 12.1 megapixel digital camera, sterilized in MeOH and returned to culture plates. To investigate whether cells affected discoloration and membrane stability, 3T3-L1 cells were seeded directly into wells with pnc-Si samples.

2.6. Cell adhesion

HUVEC and 3T3-L1 were separately seeded within cloning rings on one of five substrates in 6-well plates: PLL-coated tissue culture polystyrene, tissue culture polystyrene, glass cover slips, Teflon-fluorinated ethylene propylene (Integument Technologies, Inc., Tonawanda, NY) or pnc-Si. After seeding, cells were incubated for 5 hours in serum-supplemented media to allow attachment and then stained with CMFDA. In detail, substrates were gently rinsed in PBS to remove non-adhered cells, and the media was replaced with 6 μM CMFDA in serum-free media. After 45 minutes at 37 °C, CMFDA solution was replaced with serum-free media, and cells were incubated for another 30 minutes. Images were captured at multiple locations on each substrate with the Nikon/Cooke system described above. Microscope control and image acquisition was achieved with customized MATLAB scripts. Cells

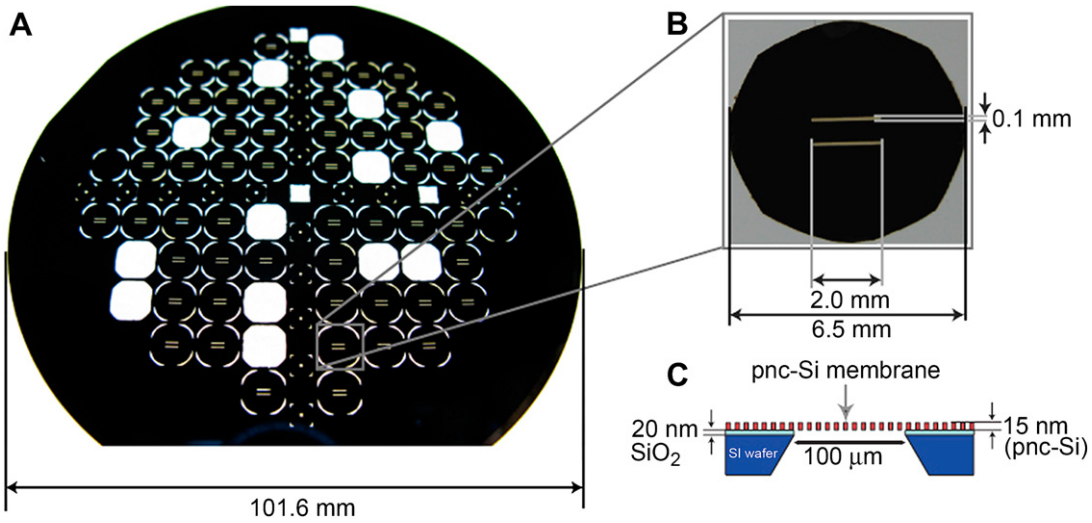

Fig. 1. Structure of pnc-Si Chips. A) Photolithographically patterned silicon wafer designed to yield approximately 80 samples, some of which are missing from this wafer. B) Each sample contains 2 approximately 2 mm × 100 μm slits with freely suspended 15 nm thin pnc-Si membranes. C) Cross sectional schematic diagram of the chip showing the 15 nm pnc-Si layer and the 20 nm sputter-deposited thermal silicon dioxide on the silicon wafer.

were counted with a MATLAB script (Supplementary Methods), and the percent adhesion was determined by comparing the MATLAB-counted cell density to the original seeding density.

2.7. Cell spreading

To measure cell spreading, HUVEC and 3T3-L1 cells were seeded inside cloning rings and onto either glass cover slips or pnc-Si samples. An open perfusion microincubator (Harvard Apparatus) was used to maintain cells at 37 °C and mineral oil was floated on top of the media to minimize evaporation. To account for lower ambient CO_2 concentrations, L15 media with 10% FBS was added (1:1, v/v) to normal cell media. Cell attachment and spreading was monitored over 5 hours by acquiring images via time lapse phase contrast imaging on the Nikon/Cooke system described above.

2.8. Cell growth kinetics

For growth kinetics experiments, HUVEC and 3T3-L1 cells were first grown to 70–80% confluence in media with or without serum. Cells were then seeded onto tissue culture polystyrene, glass or pnc-Si at low densities. To control the culture area between polystyrene, glass and pnc-Si, cloning rings were attached via vacuum grease to these substrates. Cell proliferation in media with or without serum was monitored over 4–5 days by staining cells with CMFDA and counting stained cells with MATLAB. Multiple images were taken with the Nikon microscope, and cell densities were obtained for each substrate on each day. At least three trials with triplicate measurements were carried out for each study. The data was graphed according to exponential growth kinetics

$$\frac{N}{N_0} = e^{rt}$$

where N/N_0 is the cell density normalized to the cell density on the first day, r is the per capita growth rate (slope of semilog plot) and t is time.

2.9. Cell viability

For cell viability experiments, HUVEC and 3T3-L1 were seeded onto glass cover slips or pnc-Si samples, and the culture area was constrained by cloning rings. After incubation in serum-supplemented media for 2 days, the Live/Dead Cytotoxicity Assay was used to stain cells. In detail, growth media was replaced with 2 μM calcein AM and 4 μM EthD-1 in PBS. Cells were stained in this solution for 45 minutes at 25 °C and subsequently imaged with the Nikon microscope. After imaging, a control experiment was conducted by adding 70% EtOH to cells for two hours and then repeating the live/dead assay.

2.10. Co-culture illustration

Human neutrophils were isolated from heparin-treated whole human blood [15] and then labeled for surface adhesion molecule L-selectin with either green AlexaFluor 488 (Invitrogen-Molecular Probes, Carlsbad, CA USA) or red AlexaFluor 546 tagged antibodies. Cells labeled with green fluorescent antibody were allowed to settle and adhere to the bottom surface of the pnc-Si membrane for 15 minutes in HBSS with 10 mM HEPES and 1% FBS. The pnc-Si sample was then flipped and placed into a microscope slide chamber. Cells labeled with red fluorescent antibody were plated on the top surface of pnc-Si. Using a Zeiss Axiovert 200 M epi-fluorescent microscope, z-axis slices were taken in differential interference contrast (DIC) and fluorescent channels at −4, 0 and +4 μm, where 0 μm was the estimated membrane focal plane. DIC was used as a higher resolution alternative to phase-contrast microscopy.

2.11. Data analysis

Data was reported as the mean +/− standard error. All post-acquisition image processing (overlays, pseudocolor) was conducted with ImageJ. Statistical analysis was performed using SPSS software (SPSS, Inc. Chicago, IL USA). For ANOVA, either a Kruskal–Wallis or Dunn's post-hoc analysis was performed. For all tests, significance was determined to be $p < 0.05$.

3. Results

3.1. Cell adhesion and spreading

As a prerequisite for the growth of many cell types in vitro, a surface must support cell adhesion and spreading [16–18]. Thus we began our investigation of the use of pnc-Si as a cell culture substrate by comparing the adhesion of immortalized 3T3-L1 fibroblasts and primary endothelial cells (HUVEC) on pnc-Si, tissue culture plastic, and glass. Cells were plated on these surfaces at low density and allowed to attach for five hours. The surfaces were then washed to remove loosely bound cells and the remaining cells were stained with the live cell stain CMFDA and counted via custom-built MATLAB-based scripts. For pnc-Si, counts were acquired from both supported and free-standing pnc-Si membrane areas since the surface properties of these areas are identical. Cell adhesion values were normalized to the original cell seeding density. We found there was no significant difference between HUVEC (50.45 ± 5.70%, 64.27 ± 1.26%, 65.97 ± 10.93%) or 3T3-L1 (65.14 ± 7.57%, 65.78 ± 4.39%, 74.53 ± 9.04%) adhesion to pnc-Si, glass and tissue culture plastic, respectively (Fig. 2). Poly-L-lysine (PLL)-coated tissue culture plastic was included as a positive control [19,20] and showed high cell adhesion (80.51 ± 6.32% for HUVEC, 92.31 ± 3.48% for 3T3-L1). Teflon surfaces served as negative controls and exhibited very low cell adhesion values (17.72 ± 2.12% for HUVEC, 32.53 ± 3.04% for 3T3-L1). Anchorage-dependent cells adhere optimally on wettable surfaces like tissue culture polystyrene, glass

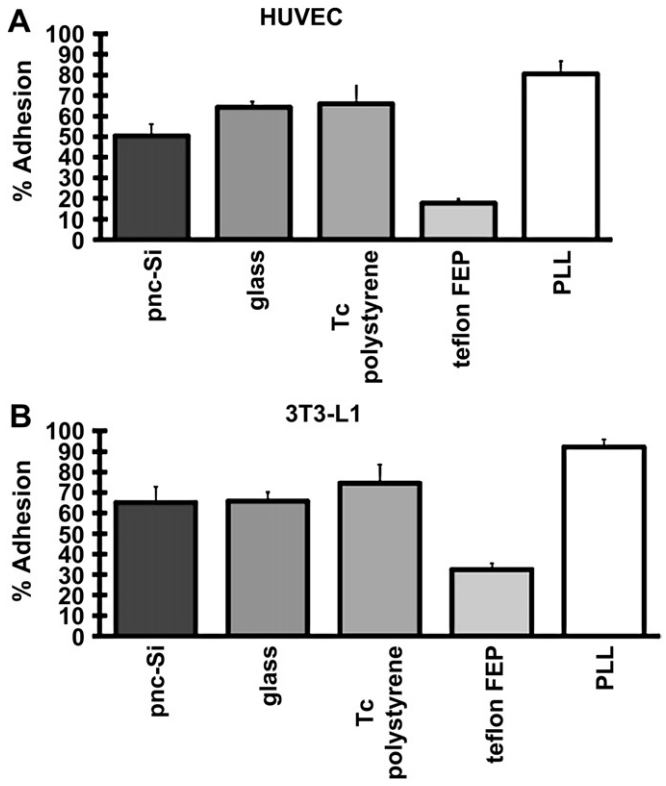

Fig. 2. Cell adhesion on pnc-Si and common substrates. Percent adhesion of HUVEC (A) and 3T3-L1 (B) cells on pnc-Si, glass and tissue culture polystyrene after 5 hours of cell culture. Teflon and PLL-coated glass were included as negative and positive controls, respectively. ($n >= 3$ with triplicate measurements). One-way ANOVA found differences in attachment of 3T3-L1/HUVEC to pnc-Si, glass, and plastic to be insignificant ($P > 0.05$). Significant differences were observed for the control experiments.

and polycarbonate [21], whereas Teflon is a hydrophobic substrate with low cell adhesion strengths [16]. The 3T3-L1 fibroblasts adhered more readily on all tested surfaces indicating these immortalized cells are more robust in culture than primary endothelial cells.

Since pnc-Si membranes are optically transparent, we were able to monitor cell spreading by time-lapse phase contrast microscopy and compare to spreading on glass coverslips (Fig. 3). Over 5 hours, 3T3-L1 and HUVEC spread on both glass and pnc-Si. Inspections within 5–10 minutes after plating (labeled 0 hours) found that both cell types had settled but not yet spread over the surface. Over the next 2 hours, cells adhered and began spreading across the substrates. After 5 hours, the elongated, fibroblast-like morphology of 3T3-L1 was evident on pnc-Si as was the cobblestone morphology typical of HUVEC [22]. Glass and pnc-Si appeared to give very similar time scales for spreading. Time-lapse phase contrast movies of 3T3-L1 and HUVEC spreading across glass and pnc-Si are available as supplementary data (Supplementary Movies 1–4).

3.2. Cell proliferation and viability

We quantified cell proliferation on pnc-Si and control surfaces by determining per capita growth rates from images of cultures grown over 4–5 days [23]. Growth in serum-free media was used as a negative control to show that the assay was sensitive to less favorable growth conditions when they existed. Our results (Fig. 4) indicate that HUVEC proliferate faster on pnc-Si (per capita growth rate: 0.0296 ± 0.0055 divisions/cell-hour) than on glass (0.0198 ± 0.0024 divisions/cell-hour) and tissue culture polystyrene (0.0223 ± 0.0036 divisions/cell-hour). 3T3-L1 cells showed statistically similar per capita growth rates on pnc-Si, glass and tissue culture plastic (0.0302 ± 0.0066, 0.0318 ± 0.0077, 0.0365 ± 0.0051 divisions/cell-hour, respectively). These values correspond to approximately 1 cell division per day for both HUVEC and 3T3-L1 on pnc-Si, which agrees with our prior work [23] examining 3T3-L1 proliferation on glass.

Cell viability on glass and pnc-Si was quantified by staining cells with live/dead fluorescent dyes and directly counting live and dead cells in fluorescent images. A microscopy-based cell viability assay was chosen because colorimetric cell viability assays based on redox reactions (e.g., Alamar Blue, MTT and XTT) give false positives on silicon substrates that also reduce the active compound. We confirmed that this problem, originally documented for porous silicon [14], also occurred with pnc-Si (data not shown). A microscopy-based viability assay showed that after 2 days of culture, both 3T3-L1 and HUVEC were nearly 100% viable on glass and pnc-Si (Fig. 5), and the cell morphologies were normal. As a control, cells were intentionally killed with EtOH to confirm that the assay reported only dead (red) signal.

3.3. Similarity to glass

Oxidation of silicon surfaces occurs within hours of exposure to atmospheric oxygen [11], thus the outer 1–2 nm of all pnc-Si chips used in our studies were assumed to be silicon dioxide or glass. Given that cells and media components interact directly with the SiO_2 coating, we anticipated that cellular behavior on pnc-Si would be quantitatively similar to glass. Indeed we found that cell adhesion, spreading, growth and viability were generally indistinguishable between pnc-Si and glass substrates. The data suggest that HUVEC adhesion was slightly lower on pnc-Si than glass, while HUVEC per capita growth rates were slightly higher. A more detailed study is needed to explore these differences, however it is possible that HUVEC were sensitive to the nanoporous surface of pnc-Si since nanoscale topographies have been shown to affect cell behavior [12,24–27]. Immortalized 3T3-L1 cells should be less sensitive to culture conditions than primary HUVEC, and indeed the growth and adhesion of 3T3-L1 were statistically indistinguishable on glass, pnc-Si or tissue culture plastic. Pnc-Si is also similar to glass in that it is optically transparent and permits fluorescence imaging without interference from autofluorescence, which occurs with most plastics. The low background in Fig. 5 in both red (Ex/Em = 528/617 nm) and green (Ex/Em = 494/517) imaging channels clearly demonstrates the lack of pnc-Si autofluorescence.

3.4. Pnc-Si dissolution in cell culture media

Porous silicon films dissolve in physiological media to produce soluble silicic acid compounds [12–14], and pnc-Si membranes exhibited the same chemical instability in cell culture media. Deterioration of the membrane manifested as a change in chip color because dissolution of the silicon layers altered the optical interference experienced by reflected light. The color progression (bottom panels, Fig. 6) was from dark blue before exposure to culture media, to purple-pink, yellow-gold, and finally silver when the underlying crystalline silicon wafer was fully exposed. We verified that these color changes correlated with membrane stability using a microparticle assay. In this assay, 15 μm polystyrene beads were deposited atop the transparent pnc-Si membranes so that their integrity could be monitored over time in a phase contrast microscope. The suspended microparticles fell out of the focal plane after 12–13 hours in serum-supplemented DMEM at room temperature, (Fig. 6 top panels; Supplemental

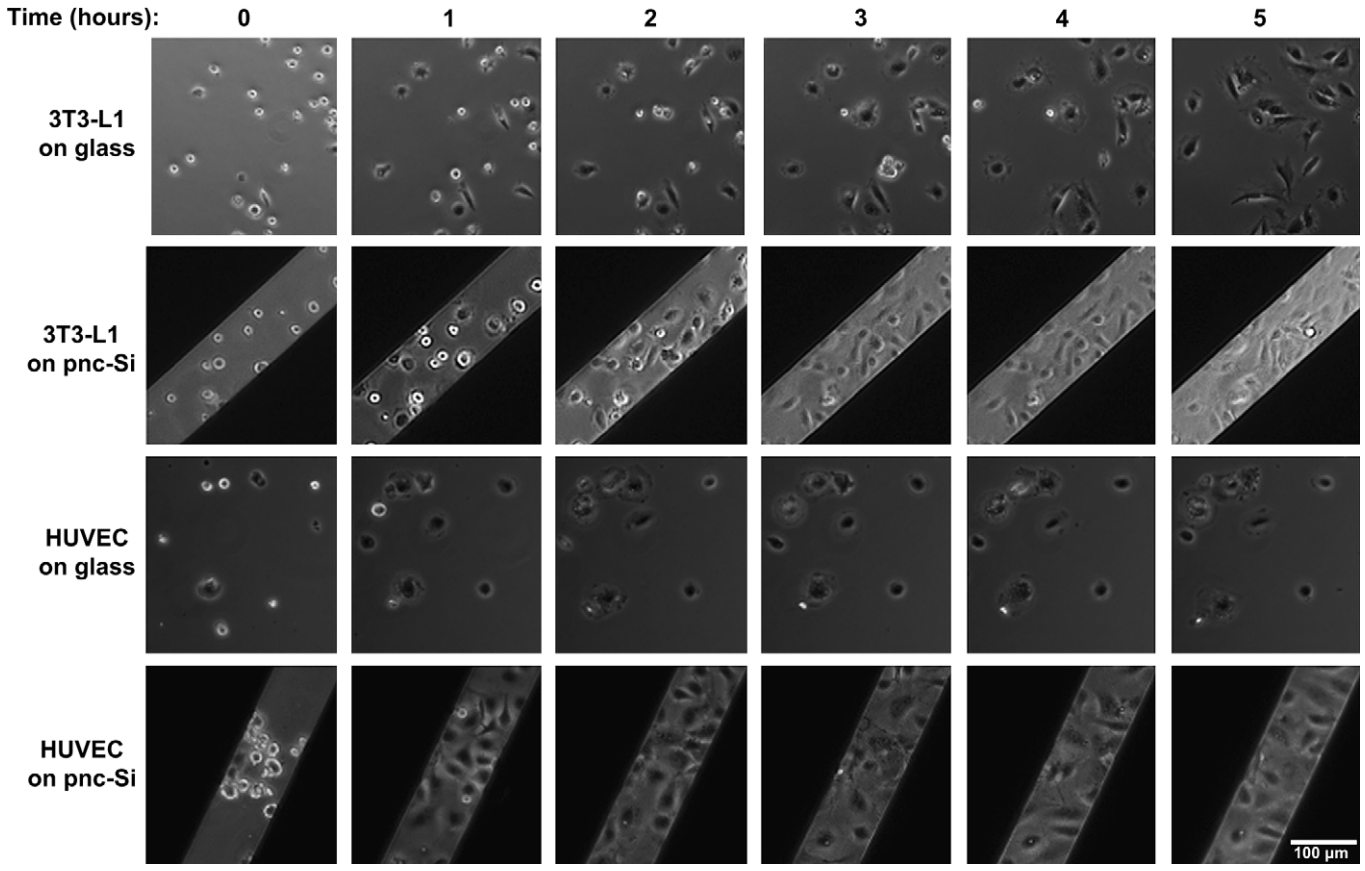

Fig. 3. Cell Spreading on pnc-Si. Phase contrast images captured from time-lapse movies of 3T3-L1 (top 2 rows) and HUVEC (bottom 2 rows) on glass and pnc-Si over 5 hours. Both cell types adhered and proliferated equally well on pnc-Si and glass. Cell morphology was also normal. The 100 μm scale bar applies to all images.

Movie 5). Pnc-Si chip color was followed simultaneously with membrane breakage and revealed that membrane breakage occurred as the chip started to discolor from blue to purple (Fig. 6 bottom panels). These studies establish that chip discoloration can be used as an indirect measure of membrane integrity.

To enable the cell culture studies described above, we needed to extend the stability of pnc-Si in cell culture media by several days. We hypothesized that heating membranes to high temperatures prior to their introduction to culture media would densify the thin native oxide and make the membranes more resistant to chemical attack. Oxide layers have been shown to enhance the chemical stability of porous silicon [14] and our own experiments found that the thick (20 nm) protective oxides present on membranes during production make membranes resistant to degradation. To densify the native oxide, chips were heated to 800 °C for 5 minutes using the same RTP unit used to induce crystals and pores in amorphous silicon. Because the treated membranes were previously crystallized at 1000 °C, we expected that a post-production thermal treatment at 800 °C would not change the membrane structure. We verified this by analyzing the pore size distributions in electron micrographs of membranes before and after post-production RTP treatments and found no significant changes in pore sizes or porosity (Fig. S1).

After post-production thermal treatment, pnc-Si membranes resisted discoloration for roughly 4 days in culture media at 37 °C, while untreated membranes showed signs of discoloration within a day under the same conditions (Fig. 7). Interestingly, the addition of cells to pnc-Si membranes appeared to accelerate the onset of discoloration so that it occurred within 3 days. This observation suggests that pH or other chemical microenvironments created by growing cells can catalyze pnc-Si dissolution. Noting that pnc-Si membranes likely began to dissolve during the last day of our 4 day cell growth studies, we reanalyzed the growth data to calculate a separate *per capita* growth rate for the first two and second two days of culture. HUVEC and 3T3-L1 cell counts were normalized to the initial cell seeding density to determine the rate for the first 2 days (HUVEC: 0.0344 ± 0.0117 divisions/cell-hour, 3T3-L1: 0.0314 ± 0.0007 divisions/cell-hour). Cell counts over the next two days were then determined and normalized to the density on the third day to determine the later growth rates (HUVEC: 0.0269 ± 0.0073 divisions/cell-hour, 3T3-L1: 0.02718 ± 0.0042 divisions/cell-hour). The growth rates calculated for the two periods were not statistically different for either cell type ($p < 0.05$), although there appeared to be a trend toward slower growth rates. Given that the cells were increasingly crowded during these growth studies, growth rates were expected to slow from contact inhibition. Still, our analysis allows us to conclude that the values reported above for *per capita* growth rates were not significantly impacted by the early stages of membrane dissolution.

3.5. Potential for co-culture applications

To illustrate the potential of pnc-Si in co-culture applications, we imaged different cell populations adhered to either side of the 15 nm thick pnc-Si membrane (Fig. 8). To create distinct cell populations, a preparation of purified human neutrophils was divided into two pools and labeled with distinct fluorescent antibodies to the abundant surface receptor L-selectin [28]. As we had found previously with glass [28], many neutrophils adhered to pnc-Si after 15 minutes of incubation in 1% FBS. Thus, after allowing 'red'

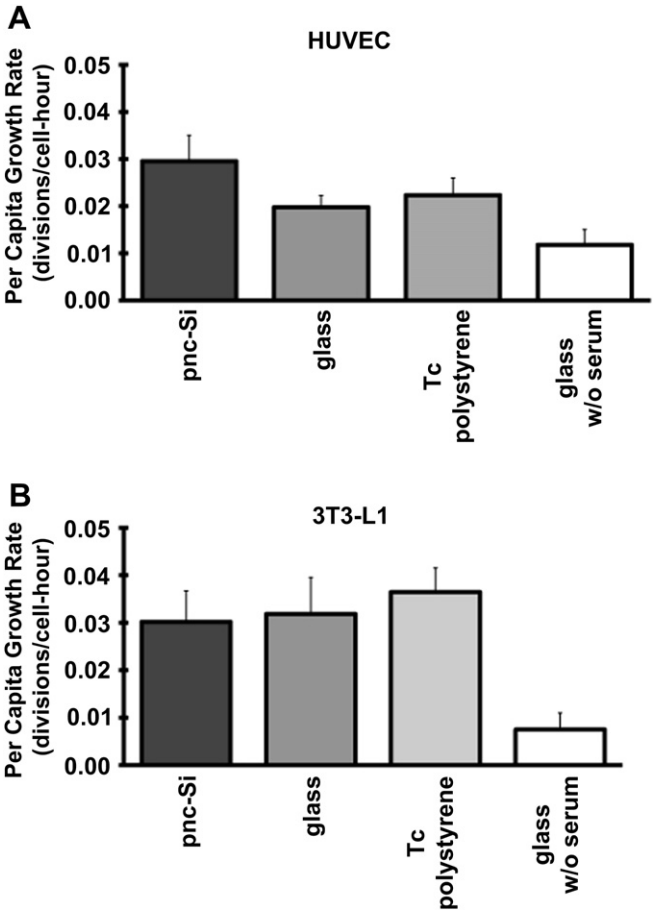

Fig. 4. Cell Growth on pnc-Si and common substrates. Per capita growth rate (number of cell divisions per cell per hour) of HUVEC (A) and 3T3-L1 (B) on glass, pnc-Si and tissue culture polystyrene over 5 days. Serum starved cells were used as a control and showed low per capita growth in both cell types. Per capita growth rates of 3T3-L1 on all 3 substrates were not significantly different ($p > 0.05$). Per capita growth of HUVEC on pnc-Si was significantly greater than on glass and plastic.

labeled neutrophils to settle and adhere on one side of the membrane, we were able to flip over the chip to allow 'green' neutrophils to adhere to the opposite side. Although no optical microscope can resolve the 15 nm membrane separating the two populations, the optical sections spaced at 4 μm in Fig. 8 clearly showed a progression where the green neutrophils were in focus beneath the membrane and the red cells were in focus above the membrane. Most significantly, the membrane itself was not visible in this sequence either as a physical structure separating the two neutrophil populations beyond their ~ 8 μm diameters [28] or as an optically visible structure that absorbs or fluoresces light in detectable quantities.

4. Discussion

Silicon has been of significant interest as a biomaterial due to its simple and scalable manufacturing, its ease of structural and chemical modification, and its potential for integration into electromechanical devices and systems [29–31]. Nanostructured materials are also of interest in biology and medicine given their potential for novel properties and applications. Here we examined the potential of a recently discovered silicon nanomaterial, porous nanocrystalline silicon (pnc-Si), to function as a cellular substrate. In quantitative studies of cellular adhesion, growth, and viability, we found that pnc-Si compared favorably to tissue culture plastic and glass. Similar results were found for both primary endothelial cells (HUVEC) and immortalized fibroblasts (3T3-L1). Given that silicon surfaces readily oxidize when exposed to atmospheric oxygen, the finding that cells interact with pnc-Si in a manner similar to glass was anticipated.

The use of silicon as a cell culture substrate has been investigated before, most often in the form of porous silicon (PSi). Cell culture has also been investigated on non-porous single crystalline silicon, silicon nitride and silicon carbide substrates [24,30,32–34]. Collectively, these prior studies have examined a wide range of cell types on silicon-based substrates and found no overt toxicity to cultures, although the ability of cells to adhere to silicon substrates varies with both cell type and surface chemistry [35,36]. Even silicic acid, which is produced when PSi naturally dissolves in biological buffers like cell culture media [12], has been found to be non-toxic at the doses experienced in cell culture on PSi [14,31,37–39].

Pnc-Si should not be confused with PSi, which is created by electrochemically etching thick wafers (50–400 μm) of single crystal silicon [40] rather than sputter deposition and annealing to create a nanocrystalline thin film. However because pnc-Si and PSi are chemically similar, it is not surprising that both forms of silicon promote favorable cell adhesion, growth and viability. Also like PSi, pnc-Si was found to dissolve in culture media in a manner that is not harmful to cells. Following procedures published by Low et al. [38], we performed an ammonium molybdate colorimetric assay and detected silicic acid in culture media after incubation with pnc-Si (not shown). However, it was difficult to rule out the possibility that the silicic acid originated from the Si support structure rather than the 15 nm-thick pnc-Si layer. Thus while we suspect pnc-Si dissolves into silicic acid in a manner similar to PSi, definitive evidence has been elusive. Importantly, the rate of substrate degradation appears to be controlled by the density of a native surface oxide since post-production annealing (~800 °C) of pnc-Si membranes extended stability in culture media from ~1 to ~4 days. The biodegradation rate of pnc-Si will need to be slowed further for some long-term cell culture applications, but short-term experiments are immediately possible. Biodegradation also creates an opportunity to create stratified tissue *in vitro* by culturing different cell types on either side of pnc-Si membranes and allowing the two populations to conjoin as the membrane dissolves.

Pnc-Si membranes may provide benefits as replacements for nanoporous polymeric membranes currently used for two major types of cell culture applications. In one type of application, polymeric membranes are used as semi-permeable substrates in assays of monolayer barrier function. In these studies, cells are grown to confluence on a 10 μm thick track-etched polymeric membrane (typically polycarbonate or polyester) suspended within a culture dish to create a 'transwell' device with upper and lower chambers. The ability of cell monolayers to regulate transport between chambers is determined with electrical resistance measurements [41,42] or by measuring the flux of small, labeled molecules [43]. For accurate measurement of barrier function, the membrane filter that separates the two chambers must offer significantly less resistance to transport than the confluent cell monolayer [5]. So the high permeability of pnc-Si could provide for more accurate measurements in these systems or enable new measurements in cases where monolayer resistances are low.

In the second application of transwell devices, filters are used to physically separate different cell types. Such arrangements are employed in the study of cell-cell communication [1,2], for three-dimensional tissue models [44] and in the creation of bioreactors requiring 'feeder' cells to support the growth of a dependent cell type [3,4]. Cell–cell communication studies often find that cells separated by transwell filters do not display the signaling that

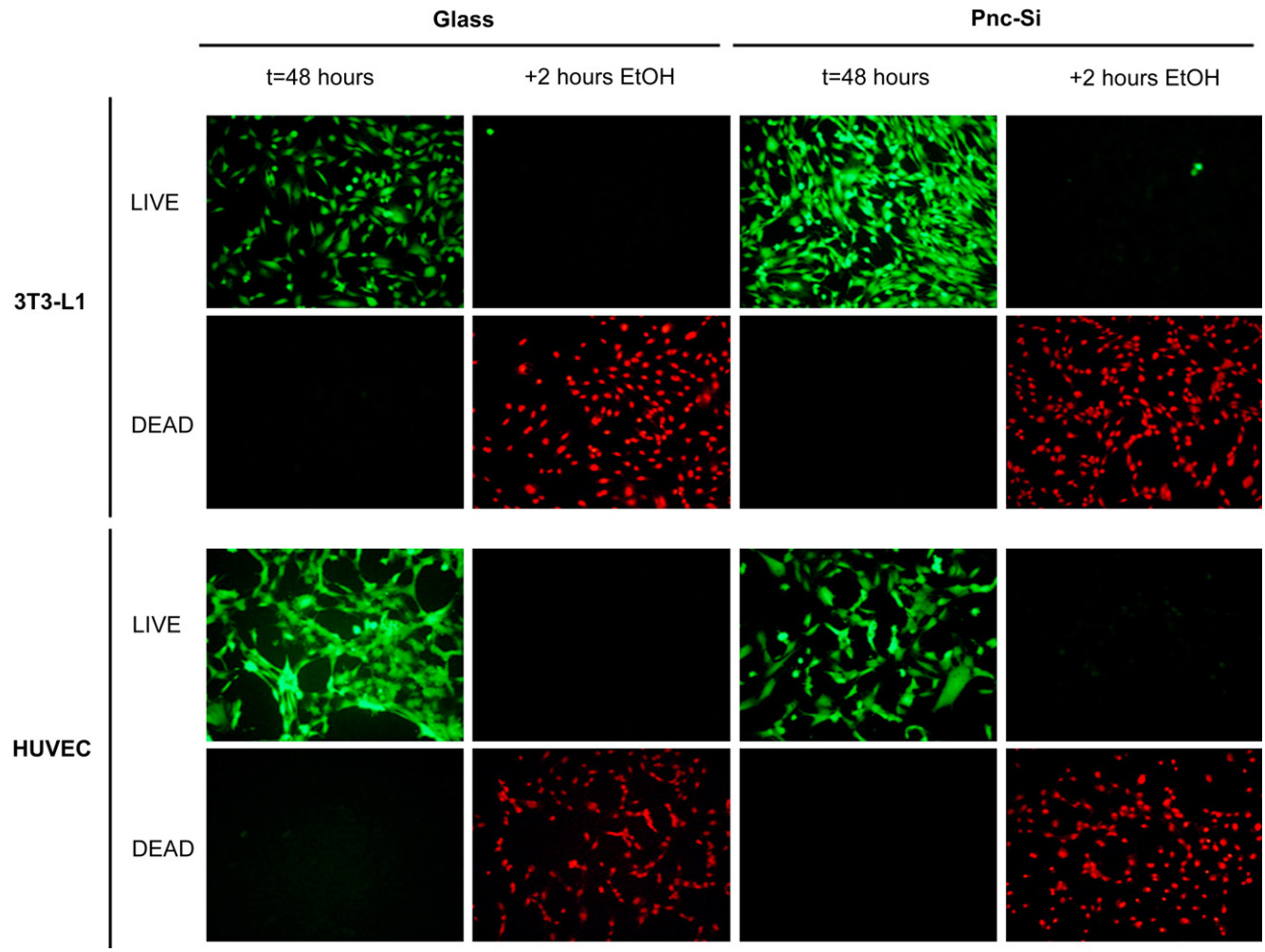

Fig. 5. Cell viability on pnc-Si and glass. 3T3-L1 and HUVEC viability on glass and pnc-Si after 2 days in vitro, as measured by the Live/Dead Cell Viability Assay (Invitrogen). Robust green fluorescence showed nearly 100% viability of both 3T3-L1 and HUVEC after 2 days. After 2 hours in 70% EtOH (positive control to kill cells), both cell types stained red by EthD-1, the dead cell stain.

occurs *in vivo*, while cells plated on the same surface do [45–48]. Such results could indicate that physical contact between the two cell types is necessary to reconstitute communication, but they may also be due to the loss of signaling molecules to polymeric membrane filters [21]. Indeed cell-cell communication *in vivo* is often mediated by secreted soluble factors that diffuse freely over distances less than 100 nm [21,49], and so the commercial transwell device is a poor mimic of *in vivo* anatomy. Pnc-Si provides an

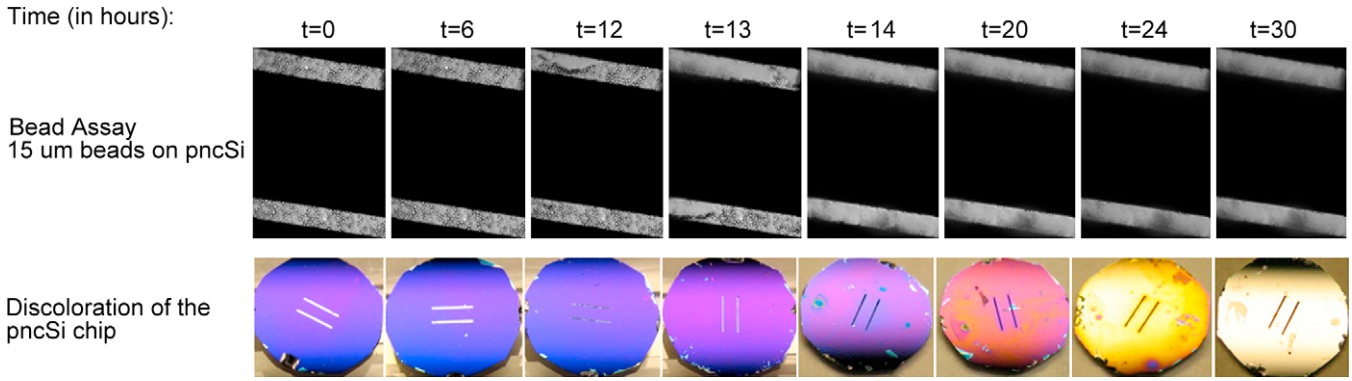

Fig. 6. Correlation between pnc-Si membrane integrity and chip discoloration. Membranes were incubated for over 30 hours in serum-supplemented DMEM at 25 °C. Top panels: 15 μm polystyrene beads settled on pnc-Si and were located via phase microscopy. At ~12 hours, the pnc-Si membrane broke and the polystyrene beads fell out of the focal plane. Bottom panels: pnc-Si chip discoloration showed a change in color from bright blue to gold over 30 hours. The initial transition from blue to purple closely matched the time point of membrane breakage.

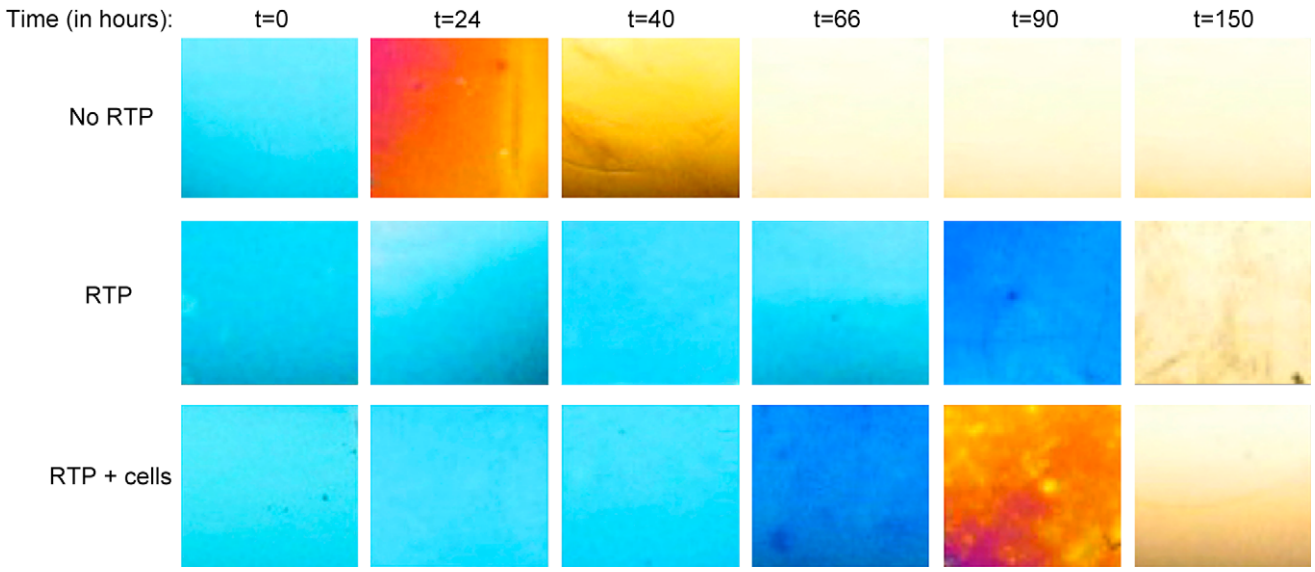

Fig. 7. Effect of post-production thermal processing on membrane stability. Treated membranes were heated for 5 minutes at 800 °C before being exposed to serum-supplemented DMEM. Without post-production annealing, pnc-Si samples discolored from blue to gold within 1 day (top). RTP delayed discoloration by at least 4 days, with discoloration noted after ~ 7 days (middle). The presence of cells (3T3-L1) along with pnc-Si increased the rate discoloration, such that the color change from blue to gold occurred between three and four days (bottom).

opportunity to create highly permeable transwells that separate cells by as little as 10 nm from each other, roughly the same thickness as cell membranes.

In addition to the potential benefits of pnc-Si as a replacement for polymer membranes in transwell devices, the silicon fabrication platform provides unique opportunities for cellular studies requiring the miniaturization of membranes. For example, arrays of pnc-Si membranes could be readily patterned to align with the wells of multiwell plates that are used for high throughput screening. Such arrays could be used to create high-density drug permeability screens with cell monolayers, or to physically isolate cells for single cell analysis while allowing them to communicate through soluble factors that pass through the membranes. The chip geometry and silicon framework of pnc-Si should allow pnc-Si membranes to serve as membrane modules in microfluidic systems since they can be readily bonded to channels made of glass, silicon or PDMS using standard techniques. In such devices, the high permeability of pnc-Si would enable the rapid delivery of test

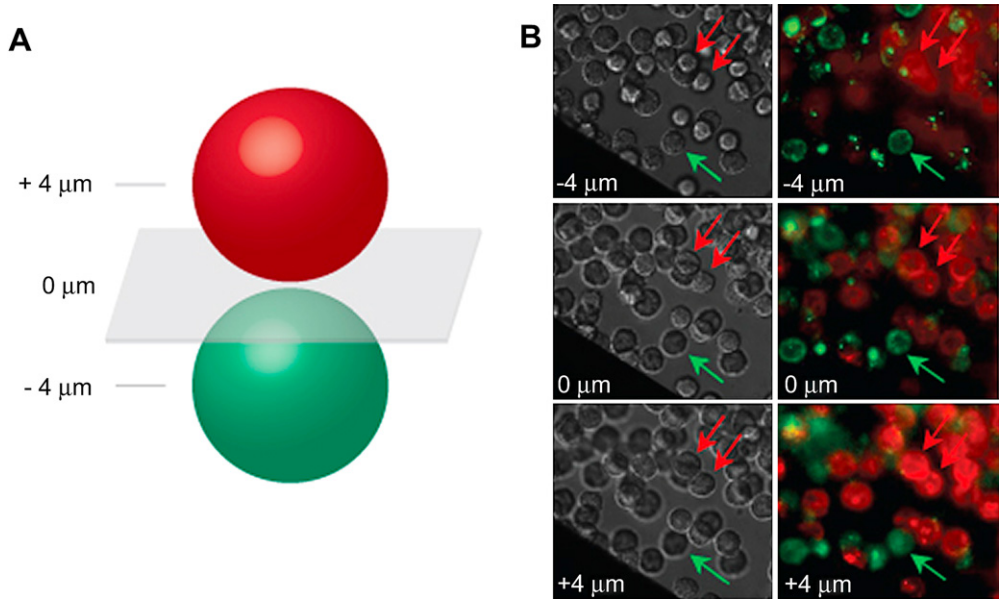

Fig. 8. Co-culture demonstration. Ultrathin pnc-Si membranes are suitable for cellular co-culture and transparent for fluorescence microscopy. (A) Schematic of experiment. Spherical human neutrophils were stained with either a green fluorescence label AlexaFluor 488 anti-CD62L or a red fluorescence label AlexaFluor 546 anti-CD62L and attached to either side of a pnc-Si Membrane. (B) Differential interference contrast (DIC; left panels) and wide-field fluorescent (right panels) images were captured at −4, 0 and +4 μm, where 0 was estimated to be the membrane focal plane. Green cells on the bottom of the membrane are in focus at −4 μm (single green arrow) and red cells on the top of the membrane are in focus at +4 μm (double red arrows).

compounds to cells through a membrane substrate, while the transparency of pnc-Si allows the monitoring of cellular responses using fluorescence and other forms of cellular microscopy.

5. Conclusions

This work establishes the feasibility of a nanoporous and ultrathin material, pnc-Si, to serve as a cell culture substrate. The adhesion, spreading, growth kinetics and viability of both an immortalized 3T3-L1 and primary HUVEC compared favorably to standard cell culture substrates by each of these metrics. Visual color changes on pnc-Si were directly correlated to nanoporous membrane stability and its biodegradation *in vitro*. Pnc-Si biodegradation exerted no cytotoxic effects and was controllable by thermally processing samples after their manufacture. Given the extraordinary permeability, molecular thinness, and transparency of pnc-Si, the material should have benefits for transwell devices used to assess transport across cell monolayers or for the establishment of cellular co-cultures. The silicon platform also opens up new avenues for devices requiring the miniaturization and integration of membranes into fluidic systems.

Acknowledgments

We would like to thank members of the Nanomembrane Research Group at the University of Rochester for their scientific and technical help. TEM images for porosity measurements were taken by Karen Bentley and HUVEC were provided by Loel Turpin from the Microbiology & Immunology Lab at University of Rochester Medical Centre. Silicon microprocessing was conducted at the Hopeman Microfabrication Facility at the University of Rochester and the Semiconductor and Microsystems Fabrication Laboratory (SMFL) at the Rochester Institute of Technology. This work was partially supported by a grant from the NYSTAR Center for Emerging and Innovative Sciences (CEIS) and SiMPore Inc. As founders of SiMPore Inc., JLM, TRG, PMF, and CSS declare a competing financial interest in this work.

Appendix. Supplementary data

Supplementary data associated with this article can be found in the online version, at doi:10.1016/j.biomaterials.2010.03.041.

Appendix

Figures with essential colour discrimination. Most of the figures in this article have parts that are difficult to interpret in black and white. The full colour images can be found in the on-line version, at doi:10.1016/j.biomaterials.2010.03.041.

References

[1] Rifas L, Avioli LV. A novel T cell cytokine stimulates interleukin-6 in human osteoblastic cells. J Bone Miner Res. 1999;14(7):1096–103.
[2] Anderson IC, Mari SE, Broderick RJ, Mari BP, Shipp MA. The angiogenic factor interleukin 8 is induced in non-small cell lung cancer/pulmonary fibroblast cocultures. Cancer Res 2000;60(2):269–72.
[3] Franco L, Zocchi E, Usai C, Guida L, Bruzzone S, Costa A, et al. Paracrine roles of NAD+ and cyclic ADP-ribose in increasing intracellular calcium and enhancing cell proliferation of 3T3 fibroblasts. J Biol Chem 2001;276(24):21642–8.
[4] Bordoni V, Alonzi T, Agrati C, Poccia F, Borsellino G, Mancino G, et al. Murine hepatocyte cell lines promote expansion and differentiation of NK cells from stem cell precursors. Hepatology 2004;39(6):1508–16.
[5] Avdeef A, Artursson P, Neuhoff S, Lazorova L, Grasjo J, Tavelin S. Caco-2 permeability of weakly basic drugs predicted with the double-sink PAMPA pKa(flux) method. Eur J Pharm Sci 2005;24(4):333–49.
[6] Matsson P, Bergstrom CA, Nagahara N, Tavelin S, Norinder U, Artursson P. Exploring the role of different drug transport routes in permeability screening. J Med Chem 2005;48(2):604–13.
[7] van Rijn C. Nano and micro engineered membrane technology. Amsterdam: Elsevier; 2004.
[8] Striemer CC, Gaborski TR, McGrath JL, Fauchet PM. Charge- and size-based separation of macromolecules using ultrathin silicon membranes. Nature 2007;445(7129):749–53.
[9] Kim E, Xiong H, Striemer CC, Fang DZ, Fauchet PM, McGrath JL, et al. A structure-permeability relationship of ultrathin nanoporous silicon membrane: a comparison with the nuclear envelope. J Am Chem Soc 2008;130(13):4230–1.
[10] Gaborski TR, Snyder JL, Striemer CC, Fang DZ, Hoffman M, Fauchet PM, et al. High performance separation of nanoparticles using ultrathin pnc-Si membranes. Nat Nanotechnol, submitted for publication.
[11] Morita M, Ohmi T, Hasegawa E, Kawakami M, Ohwada M. Growth of native oxide on a silicon surface. J Appl Phys 1990;68(3):1271–81.
[12] Anderson S, Elliott H, Wallis D, Canham L, Powell J. Dissolution of different forms of partially porous silicon wafers under simulated physioligcal conditions. Phys Stat Sol 2003;197:331–5.
[13] Anglin EJ, Cheng L, Freeman WR, Sailor MJ. Porous silicon in drug delivery devices and materials. Adv Drug Deliv Rev 2008;60(11):1266–77.
[14] Low SP, Williams KA, Canham LT, Voelcker NH. Evaluation of mammalian cell adhesion on surface-modified porous silicon. Biomaterials 2006 Sep;27(26):4538–46.
[15] Tsai MA, Frank RS, Waugh RE. Passive mechanical behavior of human neutrophils: power-law fluid. Biophys J 1993;65(5):2078–88.
[16] Freshney RI. Culture of animal cells: a manual of basic technique. New York: Wiley-Liss; 2000.
[17] Guo M, Chen J, Zhang Y, Chen K, Pan C, Yao S. Enhanced adhesion/spreading and proliferation of mammalian cells on electropolymerized porphyrin film for biosensing applications. Biosens Bioelectron 2008;23(6):865–71.
[18] Voger EA, Bussian RW. Short-term cell-attachment rates: a surface-sensitive test of cell-substrate compatibility. J Biomed Mater Res 1987;21(10):1197–211.
[19] Lakard S, Herlem G, Propper A, Kastner A, Michel G, Valles-Villarreal N, et al. Adhesion and proliferation of cells on new polymers modified biomaterials. Bioelectrochemistry 2004;62(1):19–27.
[20] Quirk RA, Chan WC, Davies MC, Tendler SJ, Shakesheff KM. Poly(L-lysine)-GRGDS as a biomimetic surface modifier for poly(lactic acid). Biomaterials 2001;22(8):865–72.
[21] Pandiyan P, Zheng L, Ishihara S, Reed J, Lenardo MJ. CD4 + CD25 + Foxp3+ regulatory T cells induce cytokine deprivation-mediated apoptosis of effector CD4 + T cells. Nat Immunol 2007;8(12):1353–62.
[22] Jaffe EA, Nachman RL, Becker CG, Minick CR. Culture of human endothelial cells derived from umbilical veins. Identification by morphologic and immunologic criteria. J Clin Invest 1973;52(11):2745–56.
[23] Bindschadler M, McGrath JL. Sheet migration by wounded monolayers as an emergent property of single-cell dynamics. J Cell Sci 2007;120:876–84.
[24] Ainslie KM, Tao SL, Popat KC, Desai TA. In vitro immunogenicity of Silicon-Based Micro- and Nanostructured Surfaces. ACS Nano 2008;2(5):1076–84.
[25] Bayliss SC, Buckberry LD, Harris PJ, Tobin M. Nature of the silicon-animal cell interface. J Porous Mater 2000;7(1–3):191–5.
[26] Bayliss SC, Heald R, Fletcher DI, Buckberry LD. The culture of mammalian cells on nanostructured silicon. Adv Mater 1999;11(4):318–21.
[27] Popat KC, Chatvanichkul KI, Barnes GL, Latempa Jr TJ, Grimes CA, Desai TA. Osteogenic differentiation of marrow stromal cells cultured on nanoporous alumina surfaces. J Biomed Mater Res A 2007;80(4):955–64.
[28] Gaborski TR, Clark Jr A, Waugh RE, McGrath JL. Membrane mobility of beta2 integrins and rolling associated adhesion molecules in resting neutrophils. Biophys J 2008;95(10):4934–47.
[29] Canham L, Reeves C, Newey J, Houlton M, Cox T, Buriak J, et al. Derivatized mesoporous silicon with dramatically improved stability in simulated human blood plasma. Adv Mater 1999;11:1505–7.
[30] Brischwein M, Motrescu ER, Cabala E, Otto AM, Grothe H, Wolf B. Functional cellular assays with multiparametric silicon sensor chips. Lab Chip 2003;3(4):234–40.
[31] Chin V, Collins BE, Sailor MJ, Bhatia SN. Compatibility of primary hepatocytes with oxidized nanoporous silicon. Adv Mater 2001;12(24):1877–80.
[32] Harris SG, Shuler ML. Growth of endothelial cells on microfabricated silicon nitride membranes for an in vitro model of the blood-brain barrier. Biotechnol Bioprocess Eng 2003;8(4):246–51.
[33] Ma SH, Lepak LA, Hussain RJ, Shain W, Shuler ML. An endothelial and astrocyte co-culture model of the blood–brain barrier utilizing an ultra-thin, nanofabricated silicon nitride membrane. Lab Chip 2005;5(1):74–85.
[34] Cappi B, Neuss S, Salber J, Telle R, Knuchel R, Fischer H. Cytocompatibility of high strength non-oxide ceramics. J Biomed Mater Res A 2009;93(1):67–76.
[35] Grattarola M, Tedesco M, Cambiaso A, Perlo G, Giannetti G, Sanguineti A. Cell adhesion to silicon substrata: characterization by means of optical and acoustic cytometric techniques. Biomaterials 1988;9(1):101–6.
[36] Kleinfeld D, Kahler KH, Hockberger P. Controlled outgrowth of dissociated neurons on patterned substrates. J Neurosci 1988;8:4098–120.
[37] Alvarez SD, Derfus AM, Schwartz MP, Bhatia SN, Sailor MJ. The compatibility of hepatocytes with chemically modified porous silicon with reference to in vitro biosensors. Biomaterials 2009;30(1):26–34.
[38] Low SP, Voelcker NH, Canham LT, Williams KA. The biocompatibility of porous silicon in tissues of the eye. Biomaterials 2009;30(15):2873–80.

[39] Mayne A, Bayliss SC, Barr P, Tobin M, Buckberry LD. Biologically interfaced porous silicon devices. Phys Stat Sol 2000;182:505–13.
[40] Zhang X. Morphology and formation of mechanisms of porous silicon. J Electrochem Soc 2004;151:856–8.
[41] Gautam N, Hedqvist P, Lindbom L. Kinetics of leukocyte-induced changes in endothelial barrier function. Br J Pharmacol 1998;125(5):1109–14.
[42] Man S, Ubogu EE, Williams KA, Tucky B, Callahan MK, Ransohoff RM. Human brain microvascular endothelial cells and umbilical vein endothelial cells differentially facilitate leukocyte recruitment and utilize chemokines for T cell migration. Clin Dev Immunol 2008;2008:384982.
[43] Hubatsch I, Eva G, Ragnarsson E, Artursson P. Determination of drug permeability and prediction of drug adsorption in Caco-2 monolayers. Nat Protoc 2007;9:2111–9.
[44] Hultman K, Bjorklund U, Hansson E, Jern C. Potentiating effect of endothelial cells on astrocytic plasminogen activator inhibitor type-1 gene expression in an in vitro model of the blood–brain barrier. Neuroscience 2010;166 (2):408–15.
[45] Ahn SE, Kim S, Park KH, Moon SH, Lee HJ, Kim GJ, et al. Primary bone-derived cells induce osteogenic differentiation without exogenous factors in human embryonic stem cells. Biochem Biophys Res Commun 2006;340(2):403–8.
[46] Ichijo H, Bonhoeffer F. Differential withdrawal of retinal axons induced by a secreted factor. J Neurosci 1998;18(13):5008–18.
[47] Kornyei Z, Szlavik V, Szabo B, Gocza E, Czirok A, Madarasz E. Humoral and contact interactions in astroglia/stem cell co-cultures in the course of glia-induced neurogenesis. Glia 2005;49(3):430–44.
[48] Schramm C, Reiter R, Solursh M. Role for short-range interactions in the formation of cartilage and muscle masses in transfilter micromass cultures. Dev Biol 1994;163:467–79.
[49] Sojka DK, Huang YH, Fowell DJ. Mechanisms of regulatory T-cell suppression – a diverse arsenal for a moving target. Immunology 2008;124(1):13–22.